ELSEVIER

Contents lists available at ScienceDirect

## Biochemical and Biophysical Research Communications

journal homepage: www.elsevier.com/locate/ybbrc



# Intracellular Doppler Spectroscopy detects altered drug response in SKOV3 tumor spheroids with silenced or inhibited P-glycoprotein



Gayatri Narayanan <sup>a</sup>, Dan Merrill <sup>c</sup>, Ran An <sup>b</sup>, David D. Nolte <sup>c</sup>, John J. Turek <sup>a,\*</sup>

- <sup>a</sup> Department of Basic Medical Sciences, Purdue University, West Lafayette, IN, 47907, USA
- <sup>b</sup> Animated Dynamics, Inc. 5770 Decatur Blvd A, Indianapolis, IN, 46241, USA
- <sup>c</sup> Physics and Astronomy, Purdue University, West Lafayette, IN, 47907, USA

#### ARTICLE INFO

Article history: Received 1 May 2019 Accepted 9 May 2019 Available online 15 May 2019

Keywords: Precision medicine Intracellular Doppler Biodynamic imaging Tumor spheroids SKOV3 P-glycoprotein MDR1

#### ABSTRACT

Intracellular Doppler spectroscopy is a form of low-coherence digital holography based upon Doppler detection of scattered light that measures drug response/resistance in tumor spheroids, xenografts, and clinical biopsies. Multidrug resistance (MDR) is one of the main causes of ineffective cancer treatment. One MDR mechanism is mediated by the MDR1 gene that encodes the drug efflux pump P-glycoprotein (Pgp). Overexpression of Pgp in some cancers is associated with poor chemotherapeutic response. This paper uses intracellular Doppler spectroscopy to detect Pgp-mediated changes to drug response in 3D tissues grown from an ovarian cancer cell line (SKOV3). The SKOV3 cell line was incrementally exposed to cisplatin to create a cell line with increased Pgp expression (SKOV3cis). Subsequently, MDR1 in a subset of these cells was silenced in SKOV3cis using shRNA to create a doxycycline inducible, Pgp-silenced cell line (SKOV3cis-sh). A specific Pgp inhibitor, zosuquidar, was used to study the effects of Pgp inhibition on the Doppler spectra. Increased drug sensitivity was observed with Pgp silencing or inhibition as determined by drug IC50s of paclitaxel-response of silenced Pgp and doxorubicin-response of inhibited Pgp, respectively. These results indicate that intracellular Doppler spectroscopy can detect changes in drug response due to silencing or inhibition of a single protein associated with drug resistance with important consequences for personalized medicine.

© 2019 The Authors. Published by Elsevier Inc. This is an open access article under the CC BY-NC-ND license (http://creativecommons.org/licenses/by-nc-nd/4.0/).

#### 1. Introduction

Biodynamic imaging (BDI) is an optical diagnostic that uses Doppler detection of light scattered from the intracellular motion of a living 3D sample to assess tissue health and to monitor processes such as mitosis [1] and apoptosis [2]. BDI can be used to study how a tissue responds to a drug or xenobiotic, and the Doppler data is used to construct drug response spectrograms by monitoring changes in intracellular motility over time [3]. The spectrograms have proven to be an accurate predictor of drug response or resistance in tumor spheroids [4], xenografts [5], and clinical biopsies [6,7]. For cancer in general, genotypic analysis is valuable, but the genetic and epigenetic complexity of tumors can result in unexpected phenotypes [8]. Predictive methods for the various cancer therapies (cytotoxins, targeted drugs, or immunotherapy) would be

E-mail address: turekj@purdue.edu (J.J. Turek).

useful to identify the patient phenotype prior to treatment or to monitor progress. Although BDI is accurate in predicting drugresponse phenotype, linkage to mechanisms of resistance is needed. One mechanism for drug resistance is the drug efflux pump P-glycoprotein (Pgp), encoded by the gene MDR1. Overexpression of this protein in some cancers is associated with poor chemotherapeutic response and with multidrug resistance due to low intracellular drug accumulation [9].

The goal of this study was to determine whether BDI could be used to detect changes in drug response mediated by Pgp. An ovarian cancer cell line (SKOV3) was used as a model system to study the effects of silencing Pgp. The native SKOV3 cell line expresses negligible levels of Pgp, but expression can be increased by incremental exposure to chemotherapy drugs such as cisplatin (SKOV3cis). The MDR1 gene was then silenced in the SKOV3cis cell line using shRNA to turn off Pgp expression (SKOV3cis-sh cell line). Pgp silencing or increased expression was confirmed by western blot and immunofluorescence. Paclitaxel is a substrate for Pgp and taxane resistance is commonly observed in multidrug resistance [10]. The drug response to paclitaxel was then compared in these

 $<sup>\</sup>ast$  Corresponding author. Purdue University, Department of Basic Medical Sciences, 625 Harrison St, West Lafayette, IN, 47907, USA.

two cell lines using a XTT cell viability assay on 2D cultures and an ATP-based cell viability assay on spheroids. These results were compared with BDI Doppler spectra. Additionally, the drug response to doxorubicin in conjunction with the Pgp inhibitor zosuquidar was studied. The experiments presented here focus on how silencing or inhibiting a single protein, Pgp, changes the *in vitro* BDI drug response in an ovarian cancer cell line. It also provides additional measures of the sensitivity of BDI for the assessment of physiological drug response.

#### 2. Material and methods

#### 2.1. Cell culture

SKOV3 cells were purchased from American Type Culture Collection (ATCC, Manassas VA). SKOV3 was grown in a 50:50 mixture of MCDB (Sigma Aldrich) and Medium 199 (Corning) media supplemented with 10% fetal bovine serum (FBS) and 100U penicillin/mL-100  $\mu$ g/mL streptomycin. To induce Pgp expression, the native SKOV3 cell line was exposed to increasing concentrations of cisplatin (up to 1  $\mu$ M) by serial passage over 5–6 weeks to create the SKOV3cis cell line. Cisplatin, paclitaxel, doxorubicin, and zosuquidar were all purchased from SelleckChem (Houston, TX) and stocks prepared in dimethylformamide (cisplatin) or dimethyl sulfoxide (DMSO). Experiments with zosuquidar (5  $\mu$ M) included a 30 min pre-incubation before adding doxorubicin.

#### 2.2. Detection of PgP by immunofluorescence and western blot

Verification of an increase in Pgp expression due to cisplatin dosing used immunofluorescence and Western blot detection. For immunofluorescence detection, cells were grown for 3 days in Nunc® Lab-Tek® 8-well Chamber Slides, fixed with methanolacetone, blocked with 3% bovine serum albumin for 30 min at room temperature, and then incubated overnight at 4 °C with 1:20 anti-Pgp (F4) primary antibody (ThermoFisher Scientific). After washing, 1:200 Dylight 488 secondary antibody (ThermoFisher Scientific) was added to the wells for 1 h in the dark followed by 1:1000 Hoechst stain and observation under a fluorescence microscope.

Changes in Pgp expression due to MDR1gene silencing was verified using western blot detection of Pgp. Spheroids, (described in Section 2.4 below), were lightly centrifuged and washed with cold phosphate buffered saline (PBS) and lysed in RIPA buffer + protease inhibitor cocktail. The samples were then kept on ice for 15 min, sonicated, and centrifuged for 20 min at 15,000 RPM. Total protein in the supernatant was calculated using the BCA Protein Assay Kit (ThermoFisher Scientific). Samples were mixed with 2x Laemmli buffer and heated at 70 °C for 10 min. SDS-PAGE was performed with 8.3% acrylamide gels and 30 µg protein per sample, then the protein was transferred onto nitrocellulose membrane. Primary antibodies used were anti-GAPDH (Thermo-Fisher Scientific) at 1:2000 and anti-p-glycoprotein (LS Bio, Seattle, WA) at 1:1000 in 3% bovine serum albumin (Sigma). Blots were first blocked with 5% milk and then incubated with primary antibody at 4 °C overnight. The membrane was washed and incubated with the corresponding secondary antibodies, goat anti-mouse HRP (ThermoFisher Scientific) and goat anti-rabbit HRP (LS Bio) at 1:2000 each at 4 °C for 1 h. Blots were then washed and incubated with SuperSignal West Pico Chemiluminescent substrate (ThermoFisher Scientific) for 5 min to develop the ECL signal. Chemiluminescence was observed with GeneSys software (SynGene, Frederick, MD).

Relative densities of western blot bands were calculated using Fiji software [11]. For each lane, densities of the band of interest were calculated as a fraction of the loading control (adjusted

relative density). Densities were normalized to the non-targeting control shRNA control sample.

#### 2.3. Gene silencing

MDR1 silencing of the SKOV3cis cell line was performed using inducible lentiviral shRNA (GE Lifesciences) as described in the Dharmacon™ SMARTvector™ Inducible Lentiviral shRNA Technical Manual. ShRNA was obtained as purified lentiviral stocks in 3 different constructs targeting MDR1: shRNA1 (CTGGCCTTCTGGTATGGGA), shRNA2 (TACAAGAATTGATGATCCT), and shRNA3 (GAGTTGGTTTGATGACCCT). The shRNA1 construct provided the most effective silencing of MDR1 based upon western blot analysis of Pgp expression. A non-targeting control (NTC) shRNA was also used as a negative control.

Transfection conditions were as follows: SKOV3cis cells were seeded at 3000 cells/well in a 96-well plate and transfected at a multiplicity of infection (MOI) of 0.8 in base DMEM with 5% FBS and 6  $\mu g/mL$  polybrene (American Bioanalytical) for 16 h at 37 °C. 100  $\mu L$  of DMEM with antibiotics and serum was added to the wells 24 h later. When the cells became confluent, they were passed into larger flasks and 1  $\mu g/mL$  doxycycline added to the medium. Red fluorescent protein (RFP) expression was determined using a fluorescent microscope. Media containing 7  $\mu g/mL$  puromycin was then used to select for successful transfectants over 5–7 days. Gene silencing confirmation experiments were carried out after 3–4 days of doxycycline exposure.

#### 2.4. Cell viability assays

The 2D IC50 for paclitaxel and doxorubicin on the cell lines was determined using an XTT Cell Proliferation Assay Kit (ATCC) as directed. 3000 cells/well were seeded in a 96 well plate in triplicate in culture medium, and the medium was replaced 24 h later containing selected drug concentrations. Control wells contained 0.1% DMSO. Plates were incubated for 72 h at 37 °C. XTT solution with activation reagent was then added to wells and incubated for 2.5 h at 37 °C. Absorbance was read in a plate reader at 475 and 660 nm using SoftMax Pro 6 (Molecular Devices, San Jose, CA). The paclitaxel IC50 for uninduced SKOV3cis was compared to Pgpsilenced SKOV3cis. The effect of zosuquidar on doxorubicin IC50 for SKOV3cis was also determined.

To prepare for biodynamic imaging of 3D tissues, 3D cell viability and test drug concentrations were selected using the CellTiterGlo 3D Cell Viability Assay (Promega, Madison, WI) as directed. SKOV3 spheroids for experiments were created using spheroid microplates (Corning) for 4–5 days with media replenished every 2 days. Initial seeding was at 10,000 cells per well and final spheroid diameter was 300–400  $\mu m$ . Media containing the drugs at varying concentrations was added and assayed at 9 or 72 h. The 9 h time point was chosen to match the BDI experiments that monitor drug response for a minimum of 9 h. CellTiterGlo reagent was added to each well, including pure ATP standards, shaken, and incubated for 30 min. The relative luminescence units (RLU) were measured using SoftMax Pro 6. The luminescence is proportional to amount of ATP and cell viability. All percent viabilities were calculated by dividing the test result with the control result times 100%.

#### 2.5. Tissue Doppler imaging

Intracellular Doppler spectroscopy is performed using a biodynamic imaging optical system composed of a low-coherence light source, a Mach-Zehnder interferometer configuration and off-axis digital holography performed on a Fourier optical plane with

numerical image reconstruction. The system detects dynamic speckle across a field of view of approximately 1 mm. The dynamic speckle is the result of multiple beat frequencies of partial waves scattered by moving intracellular constituents in 3D tissue. The time series of the speckle intensity is analyzed into fluctuation power spectra. Relative changes in spectral density are displayed as drug-response spectrograms, as shown in Fig. 3a and b). The spectral response to paclitaxel was compared for SKOV3cis vs SKOV3-cis-sh (Pgp silenced). The spectral response to doxorubicin was compared for SKOV3cis with and without the Pgp inhibitor zosuguidar (5 µM). Spheroids grown as described above (Section 2.4) were immobilized in a thin layer of 1% low-gel temperature agarose (SigmaAldrich, St. Louis, MO) made up in basal growth medium in 96-well plates and then covered in a layer of complete growth medium. The plates were sealed with a permeable membrane (Breathe Easy, Diversified Biotech, Dedham, MA), and placed on the 37 °C heated stage of the instrument. BDI baseline spectra were collected over 4h periods and then the drugs paclitaxel  $(10\mu\text{M})$  or doxorubicin  $(10\,\mu\text{M}) \pm zosuquidar$  added and the drug response spectra collected over a 9h period. The carrier 0.1% dimethyl sulfoxide (DMSO) was used as negative control.

The time-frequency drug-response spectrograms for each sample were analyzed using feature masks that capture changes in intracellular dynamics. Specific intracellular mechanisms are separated by the wide frequency range of the spectral analysis with low frequencies (10 mHz–100 mHz) associated with cell shape changes, mid frequencies (100 mHz–1 Hz) associated with membrane processes and nuclear motions, and high frequencies (1 Hz–10 Hz) associated with organelle and vesicle transport. Spectral features include overall enhancement/suppression of

activity across all frequencies; localized low, mid and high frequencies; red shifts (increased lower frequencies) or blue shifts (increased higher frequencies); and the time dependence in response to the applied treatment. A description of the Doppler instrument and these feature vectors can be found in previous publications on biodynamic imaging [1–3].

#### 2.6. Statistical analysis

Drug resistance assays were performed in three sets of triplicates. JMP 12 software was used to graph and determine IC50 values and a Student's *t*-test was performed to determine statistical significance between two treatment groups. The time-frequency feature biomarkers were analyzed with the two-sample Kolmogorov-Smirnov test using MATLAB to determine if there was a significant spectral difference between the treatments. A p-value < 0.05 indicated statistical significance.

#### 3. Results

#### 3.1. Pgp expression and silencing

The parental SKOV3 cell line expressed negligible levels of Pgp, but successive exposure to cisplatin caused the SKOV3 cells to express more Pgp as detected by immunofluorescence (Fig. 1a). The Pgp-upregulated SKOV3cis line was then transfected with MDR1 shRNA and Pgp levels detected using Western blot analysis. When doxycycline was added to the media, the shRNA was induced and Pgp expression was effectively reduced. Uninduced SKOV3cis (no doxycycline, thus no shRNA expression) had Pgp levels similar to

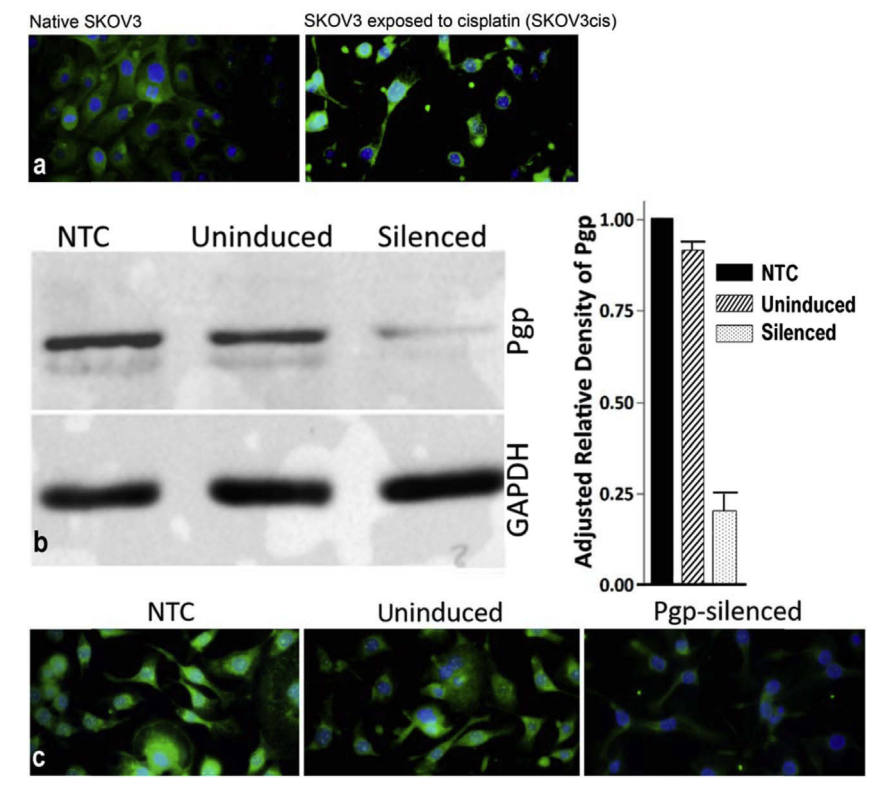


**Fig. 1.** Detection of Pgp levels. a) Upregulation of Pgp expression due to cisplatin exposure detected by immunofluorescence. Pgp distribution is shown in green nuclei are shown in blue (Hoechst stain). Following fixation and blocking, cells were incubated with 1:20 anti-Pgp (F4) primary antibody (ThermoFisher Scientific) and 1:200 Dylight 488 secondary antibody (ThermoFisher Scientific). b) Western blot analysis of the SKOV3cis cell line transfected with a non-targeting control (NTC) shRNA, and an MDR1 shRNA inducible with doxycycline. c) Average relative density values of the Pgp band derived from 3 independent Western blots verified significant reduction in Pgp expression upon doxycycline induction. Error bars represent standard error of the mean. d) Immunofluorescence verification of Pgp silencing showing Pgp fluorescence levels in NTC, uninduced, and silenced SKOV3cis cells.

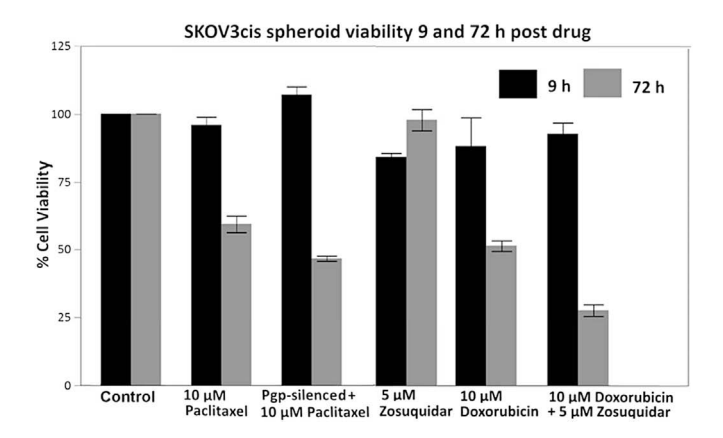


**Fig. 2.** ATP assay for measurement of 3D spheroid viabilities at 9 and 72 h post drug treatment. SKOV3cis spheroids with and without Pgp were dosed with paclitaxel for 9 and 72 h SKOV3cis spheroids were treated with doxorubicin with and without the Pgp inhibitor zosuquidar. Error bars represent standard error of the mean (N=3). Experimental viabilities are normalized to the negative control  $(0.1\% \ DMSO)$ .

the line transfected with NTC control shRNA, as expected (Fig. 1b and c). These results were further verified by immunofluorescence. The induced shRNA SKOV3cis line has decreased Pgp as compared to the NTC and uninduced cell lines (Fig. 1d).

# 3.2. Effect of Pgp silencing or inhibition on sensitivity to paclitaxel and doxorubicin

2D drug sensitivities measured with the XTT assay were as follows. The uninduced SKOV3cis cell line had an IC50 for paclitaxel of  $20.6\pm1.0$  nM. The IC50 was significantly reduced (p <0.05) for the PgP-silenced SKOV3cis to  $10.8\pm1.9$  nM. For doxorubicin, the SKOV3cis cells had an IC50 of  $99.3\pm12.3$  nM. Zosuquidar significantly reduced (p <0.05) the IC50 for doxorubicin to  $57.6\pm8.7$  nM. Exposure of SKOV3cis cells to zosuquidar alone at  $5\,\mu\text{M}$  alone had no effect of cell viability. These experiments demonstrate that silencing or inhibition of Pgp increased drug sensitivity in these cell lines.

Initial spheroid dosage experiments found that results comparable to the 72 h 2D XTT assay required higher drug concentrations. Fig. 2 shows that the reduction in cell viability to paclitaxel and doxorubicin was greatest in Pgp silenced or inhibited spheroids. The results of the ATP assay after 9 h drug exposure did not show any differences in cell viability, indicating that this assay lacks the sensitivity at this early drug exposure timepoint. This is an important comparison with the Doppler spectra, which have proven to be sensitive indicators of early (within hours) drug response in spheroids or clinical biopsies.

#### 3.3. Biodynamic imaging

Fig. 3a shows average drug-response spectrograms for Pgp-expressing SKOV3cis spheroids compared to Pgp-silenced SKOV3cis-sh spheroids after 10  $\mu$ M paclitaxel treatment. The x-axis on the spectrograms indicates intracellular speed detection by Doppler. The speed  $\nu=f\lambda/2n$ , where f is the detected Doppler frequency,  $\lambda=840$  nm is the wavelength of the light source and n = 1.35 is the refractive index of the 3D tissue. The y-axis is time, and the color bar indicates percent change in intracellular speed (green = no change, blue = decrease or suppression, red = increase or enhancement). The effects of DMSO and 1  $\mu$ g/mL doxycycline have been subtracted. Paclitaxel causes a strong mid-speed suppression (0.1–1  $\mu$ m/s), seen as blue. The same treatment produces a different spectrogram when Pgp is silenced. The mid-speed suppression

remains, but there is also a strong activation at low (<0.1  $\mu m/s$ ) speeds and slighter activation high speeds (>10  $\mu m/s$ ) seen as yellow on the spectogram. This spectral pattern has previously been shown to correspond with apoptosis [2]. Apoptosis is energetic and consistently shows enhanced activity at high frequencies (organelle and vesicle transport) and low frequencies (apoptotic body formation) in these BDI spectrograms. Fig. 3b shows the average doxorubicin spectrograms of SKOV3cis spheroids with and without the specific Pgp inhibitor zosuquidar. The effects of DMSO have been subtracted. When treated with doxorubicin only, the spheroids show suppressed motion in the high-speed range and activation in the low-speed range. However, when zosuquidar is added, there is enhanced suppression in the high-speed (organelle and vesicle) range (>1  $\mu$ m/sec) as indicated by a darker blue color and this change occurs at an earlier time point.

The differences in the spectograms were quantified by 6 different feature-vector biomarkers to determine the significant differences. The time-frequency biomarkers were used in the twosample Kolmogorov-Smirnov (K-S) test (Fig. 3c and d). Fig. 3c shows the differences in the distribution of frequency biomarker values between Pgp-expressing SKOV3cis and silenced SKOV3cis-sh post drug. Fig. 3d shows the differences in the distribution of doxorubicin drug-response frequency biomarker values between SKOV3cis with and without the inhibitor zosuquidar. Table 1 contains the K-S test statistic and the associated p values for all experiments. The most significant biomarkers for silencing of paclitaxel are so-called "red-shifting" (sine-dipole) and "Doppler edge-burning" (cosinedipole) [12]. The most significant biomarkers for inhibition of doxorubicin by zosuguidar are overall suppression of activity. Inhibition of Pgp by zosuguidar is a significantly weaker effect for doxorubicin response than gene silencing for paclitaxel, although both effects are statistically significant (p < 0.05). These results confirm the significant differences in spectral drug response to paclitaxel when Pgp expression is silenced and to doxorubicin when Pgp is inhibited.

#### 4. Discussion

In summary, biodynamic imaging (BDI) based upon Doppler spectroscopy of intracellular motion detects significant differences in the physiological drug response of a Pgp-expressing ovarian cancer SKOV3 cell line when Pgp is silenced or inhibited. This is the first use of BDI to compare drug responses of samples with differing expression levels of a single protein. With paclitaxel, a common drug for treatment of ovarian cancer, silencing Pgp shifts the BDI spectrogram pattern to a characteristic apoptotic pattern. The BDI spectrum for Pgp-silenced spheroids dosed with paclitaxel shows activation in the low and high ends of the frequency spectrum. These shifts correspond to changes in active transport of vesicles (high frequency) and formation of apoptotic bodies (low frequency). This suggests that silencing Pgp allows more paclitaxel to accumulate within the cell and to initiate apoptosis. This shift in the paclitaxel spectrum indicating increased drug sensitivity corresponds to the decreased IC50 noted in the 2D cytotoxicity assay and 72 h 3D ATP assay. Significantly, the results highlight the sensitivity of BDI to changes in drug-induced intracellular dynamics that are not detectable by a more traditional cell viability assay.

Doxorubicin is another substrate for Pgp [13]. Inhibiting Pgp with zosuquidar resulted in enhancement of the effects of the drug as visualized by enhanced high-frequency suppression that is measurable at an earlier time point than using conventional assays. These visual changes observed in the time-frequency spectrograms were confirmed by K-S analysis having statistical significance for several frequency biomarkers.

The use of BDI for drug sensitivity testing has basic science

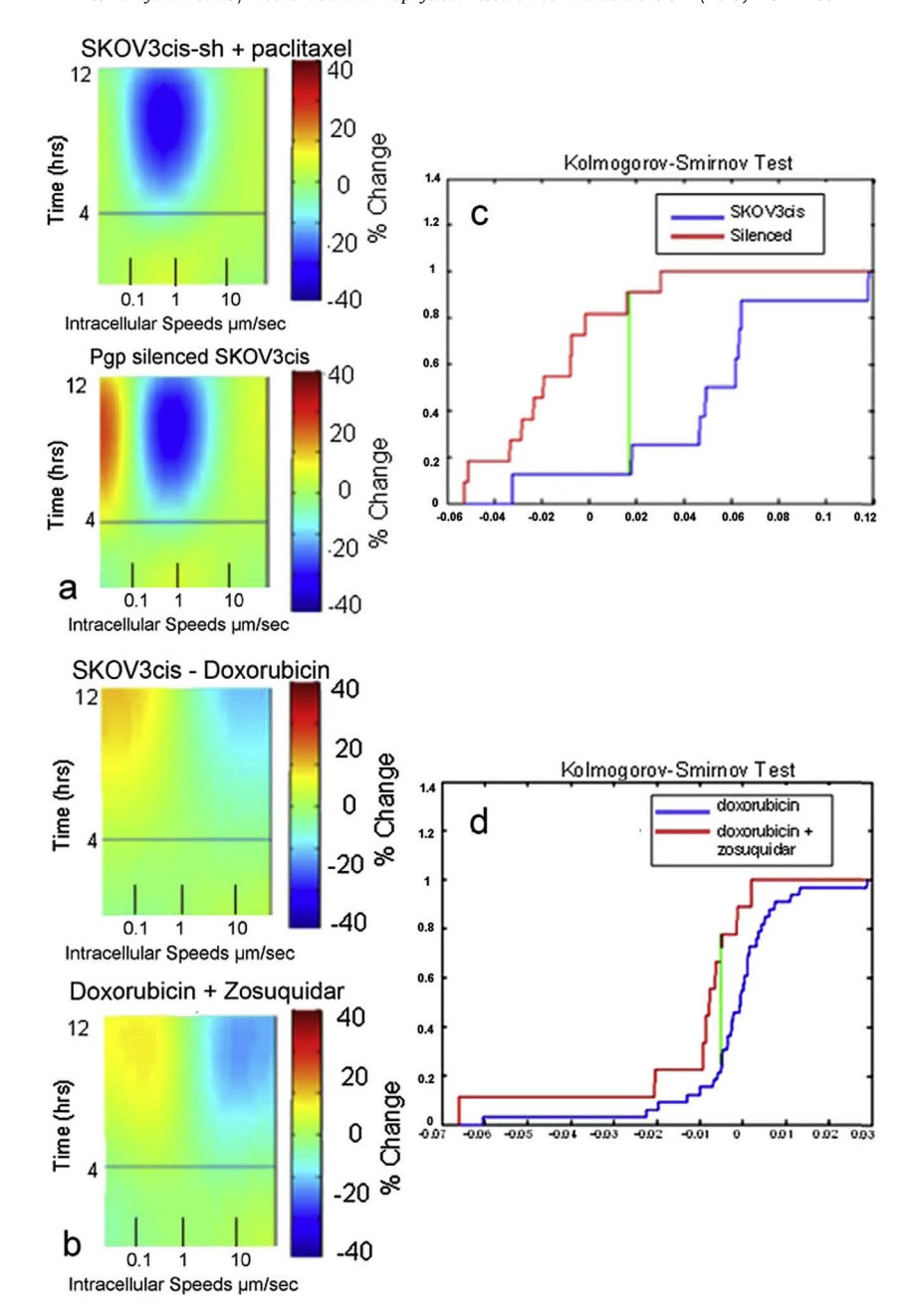


**Fig. 3.** a) Average paclitaxel (10  $\mu$ M) drug-response spectrograms for Pgp expressing SKOV3*cis*-sh spheroids vs Pgp-silenced SKOV3*cis*-sh spheroids. b) Average doxorubicin (10  $\mu$ M) response spectrograms for SKOV3*cis* vs SKOV3*cis* + zosuquidar (5  $\mu$ M). c) A two-sample Kolmogorov-Smirnov test showing significant differences in the distribution of the BDI biomarker values between Pgp-expressing and silenced SKOV3*cis* post drug. d) A two-sample Kolmogorov-Smirnov test showing differences in the distribution of BDI biomarker values between SKOV3*cis* and SKOV3*cis* + zosuquidar.

applications such as phenotypic drug screening using 3D tissues. Previous work has shown that phenotypic hierarchical clustering of spectral changes could be compared to 2D high-content analysis (HCA) screening methods, but the BDI performed in 3D tissues showed differences approximately 30% of the time [4]. Identifying new or unexpected phenotypes that could be missed by 2D HCA screening methods has value in early-stage drug development. The ability to detect a change in drug response due to silencing or inhibition of a single protein indicates that BDI could be valuable for targeted screens where drug analogs are tested as well as enhancing our understanding of genotype-phenotype relationships. The ability to rapidly identify responder/non-responder

patients for a given drug therapy is currently being explored in human trials and results from naturally occurring canine B-cell lymphoma patients [6,7] show promise that BDI will have applications for human personalized medicine.

### **Conflicts of interest**

The authors, Ran An, David D. Nolte, John J. Turek have a financial interest in a company (Animated Dynamics, Inc) that is commercializing biodynamic imaging technology.

**Table 1**Kolmogorov-Smirnov test statistic values per BDI feature vector (biomarker) group. N for each drug treatment is given. P-values less than 0.05 are indicated with \*. Pooled biomarkers were (1) All frequencies over the time course of the drug exposure, (2) All frequencies but with a time dependency of 50% early and 50% late. (3) Sine of the dipole frequencies (high vs low), (4) Cosine of the dipole frequencies (high, medium, and low), (5) High frequency band, (6) Low frequency band.

| SKOV3cis-sh Pgp positive (N = 8) vs SKOV3cis-sh Pgp Silenced (N = 11) |                   |         | SKOV3cis  10 $\mu$ M Doxorubicin (N = 39) vs 10 $\mu$ M Doxorubicin + Zosuquidar (N = 9) |         |
|---|-------------------|---------|--|---------|
| 10 μM paclitaxel  |                   |         |  |         |
| Frequency Biomarker   | KS Test Statistic | p-value | KS Test Statistic  | p-value |
| 1 - All frequencies   | 0.25              | 0.56    | -0.535   | 0.015*  |
| 2 —All frequencies- early/late  | -0.375            | 0.272   | -0.484   | 0.032*  |
| 3 – Sine of dipole (high and low frequencies)                         | -0.78             | 0.003*  | 0.202  | 0.551   |
| 4 – Cosine of dipole (high, medium, and low frequencies               | -0.75             | 0.005*  | 0.2525   | 0.394   |
| 5 — High frequency band   | 0.318             | 0.391   | -0.212   | 0.518   |
| 6 — Low frequency band  | 0.477             | 0.121   | -0.272   | 0.337   |

#### Acknowledgements

This research was supported by grants from the NIH National Institute of Biomedical Imaging and Bioengineering 1R01EB016582-01 and National Science Foundation 1263753-CBET. We would like to thank Ingrid Schoenlein and Dr. Zhibin Cui for their assistance.

#### Appendix A. Supplementary data

Supplementary data to this article can be found online at https://doi.org/10.1016/j.bbrc.2019.05.072.

#### References

- H. Sun, D. Merrill, R. An, J. Turek, D. Matei, D.D. Nolte, Biodynamic imaging for phenotypic profiling of three-dimensional tissue culture, J. Biomed. Opt. 22 (2017) 16007.
- [2] D.D. Nolte, R. An, J. Turek, K. Jeong, Tissue dynamics spectroscopy for phenotypic profiling of drug effects in three-dimensional culture, Biomed. Opt. Express 3 (2012) 2825–2841.
- [3] D.D. Nolte, R. An, J. Turek, K. Jeong, Holographic tissue dynamics spectroscopy, J. Biomed. Opt. 16 (2011) 087004.
- [4] R. An, D. Merrill, L. Avramova, J. Sturgis, M. Tsiper, J.P. Robinson, J. Turek, D.D. Nolte, Phenotypic profiling of Raf inhibitors and mitochondrial toxicity in 3D tissue using biodynamic imaging, J. Biomol. Screen 19 (2014) 526–537.
- [5] D. Merrill, R. An, H. Sun, B. Yakubov, D. Matei, J. Turek, D. Nolte, Intracellular

- Doppler signatures of platinum sensitivity captured by biodynamic profiling in ovarian xenografts, Sci. Rep. 6 (2016) 18821.
- [6] M.R. Custead, R. An, J.J. Turek, G.E. Moore, D.D. Nolte, M.O. Childress, Predictive value of ex vivo biodynamic imaging in determining response to chemotherapy in dogs with spontaneous non-Hodgkin's lymphomas: a preliminary study, Converg. Sci. Phys. Oncol. 1 (2015).
- [7] H. Choi, Z. Li, H. Sun, D. Merrill, J. Turek, M. Childress, D. Nolte, Biodynamic digital holography of chemoresistance in a pre-clinical trial of canine B-cell lymphoma, Biomed. Opt. Express 9 (2018) 2214–2228.
- [8] V. Almendro, Y.K. Cheng, A. Randles, S. Itzkovitz, A. Marusyk, E. Ametller, X. Gonzalez-Farre, M. Munoz, H.G. Russnes, A. Helland, I.H. Rye, A.L. Borresen-Dale, R. Maruyama, A. van Oudenaarden, M. Dowsett, R.L. Jones, J. Reis-Filho, P. Gascon, M. Gonen, F. Michor, K. Polyak, Inference of tumor evolution during chemotherapy by computational modeling and in situ analysis of genetic and phenotypic cellular diversity, Cell Rep. 6 (2014) 514–527.
- [9] G. Housman, S. Byler, S. Heerboth, K. Lapinska, M. Longacre, N. Snyder, S. Sarkar, Drug resistance in cancer: an overview, Cancers 6 (2014) 1769–1792.
- [10] M.M. Gottesman, T. Fojo, S.E. Bates, Multidrug resistance in cancer: role of ATP-dependent transporters, Nat. Rev. Canc. 2 (2002) 48–58.
- [11] J. Schindelin, I. Arganda-Carreras, E. Frise, V. Kaynig, M. Longair, T. Pietzsch, S. Preibisch, C. Rueden, S. Saalfeld, B. Schmid, J.Y. Tinevez, D.J. White, V. Hartenstein, K. Eliceiri, P. Tomancak, A. Cardona, Fiji: an open-source platform for biological-image analysis, Nat. Methods 9 (2012) 676–682.
- [12] Zhe Li, John Turek, Shadia Jalal, Michael Childress, David D. Nolte, Doppler fluctuation spectroscopy of intracellular dynamics in living tissue, J. Opt. Soc. Am. A 36 (2019) 665–677.
- [13] T. Yamagishi, S. Sahni, D.M. Sharp, A. Arvind, P.J. Jansson, D.R. Richardson, P-glycoprotein mediates drug resistance via a novel mechanism involving lysosomal sequestration, J. Biol. Chem. 288 (2013) 31761–31771.